



## Design, Synthesis, Characterization, Molecular Docking Studies, *In vitro* and *In vivo* Cervical Cancer Activity of Novel N-Substituted Pyrazole Derivatives

T. SUDHA<sup>1,\*</sup>, D. MAHALAKSHMI<sup>2</sup> and P. KUMAR NALLASIVAN<sup>3</sup>

<sup>1</sup>Department of Pharmaceutical Chemistry and Analysis, School of Pharmaceutical Sciences, Vels Institute of Science, Technology and Advance Studies (VISTAS), Pallavaram, Chennai-600117, India

<sup>2</sup>Department of Pharmaceutical Chemistry, Saveetha College of Pharmacy, Saveetha Institute of Medical and Technical Sciences, Chennai-600105, India

<sup>3</sup>Department of Pharmaceutical Chemistry, Karpagam Academy of Higher Education, Coimbatore-641021, India

\*Corresponding author: E-mail: [jvchrsty@yahoo.co.in](mailto:jvchrsty@yahoo.co.in)

Received: 26 May 2024;

Accepted: 18 July 2024;

Published online: 30 September 2024;

AJC-21755

The aim of this study is to design, synthesize, characterize few novel N-substituted pyrazole derivatives and evaluated for their anticancer capabilities; these compounds were selected based on their ability to inhibit the HPV E6 protein. The IR, <sup>1</sup>H & <sup>13</sup>C NMR, mass spectral and elemental analysis were used to determine the structural details of the newly synthesized substances. The molecular docking was performed using Auto Dock Vina, and the protein-ligand interaction was analyzed using Discovery Studio. The sulforhodamine B (SRB) assay was used to determine the *in vitro* anticancer activity against the HeLa cell line. Body weight analysis, mean survival time and % increase in life span approaches were used to assess *in vivo* anticancer effectiveness in Swiss albino mice bearing Dalton's Lymphoma Ascites (DAL) tumor model. Synthesized compounds have excellent docking energies, according to docking experiments. Compounds **I**, **II** and **III** were selected for anticancer activity *in vivo* DAL-bearing mice based on the findings of their *in vitro* and SRB assays exhibiting the antiproliferative activity. Pyrazole derivatives, compounds **I** and **III**, demonstrated significant potential as anticancer agents.

**Keywords:** Pyrazole derivatives, Molecular docking, Cervical cancer, Cancer cell line, *In vivo* anti-tumour activity.

### INTRODUCTION

Cancer is a significant global issue and ranks as the second leading cause of mortality in developed countries [1]. Some commercially available chemotherapy drugs have properties that render them ineffective against cancer [2]. Considering the severity of cancer and the fact that current medicines have limited efficacy, developing novel, effective cancer treatments is a primary focus of medicinal chemistry. Although there have been advancements in the use of chemotherapy medicines with certain individuals, the challenging endeavor of discovering novel anticancer treatments remains crucial [3-5]. The pharmaceutical industry is facing a decline in profitability, leading to significant reductions in medicine development and research efforts in recent years [6]. However, one of the prevailing methods to develop novel medications involves modifying the molecular structure of a promising lead compound [7].

The pyrazole ring is a significant structure in pharmaceutical and combinatorial chemistry research because it plays a vital role in physiologically active compounds [8,9], including therapeutic molecules like pyrazofurin, celecoxib, and several others. In fact, it has been shown that a number of pyrazole derivatives have anti-inflammatory, antimicrobial, antiviral, antidiabetic, anti-androgenic, painkiller and antioxidant effects [10,11].

The objective of the investigation in the present scenarios is to find a novel heterocyclic compound that exhibits favorable biological activity and minimal adverse effects. Consequently, we became intrigued by the prospect of synthesizing several novel N-substituted pyrazole molecules. Based to this view, the development of new pharmacologically active compounds is essential for effectively fighting cancer cells. After conducting a thorough examination of the available literature, we have determined that the HPV E6 [12] protein is the most suitable target for the drug design and synthesis efforts. A novel set of

pyrazole derivatives (I-IV) is designed, synthesized and subjected to molecular docking experiments with an HPV E6 protein. The cytotoxic activity of these derivatives is evaluated against the HeLa cell line, and an *in vivo* research is conducted utilizing the Ehrlich Ascites Carcinoma (EAC) models.

## EXPERIMENTAL

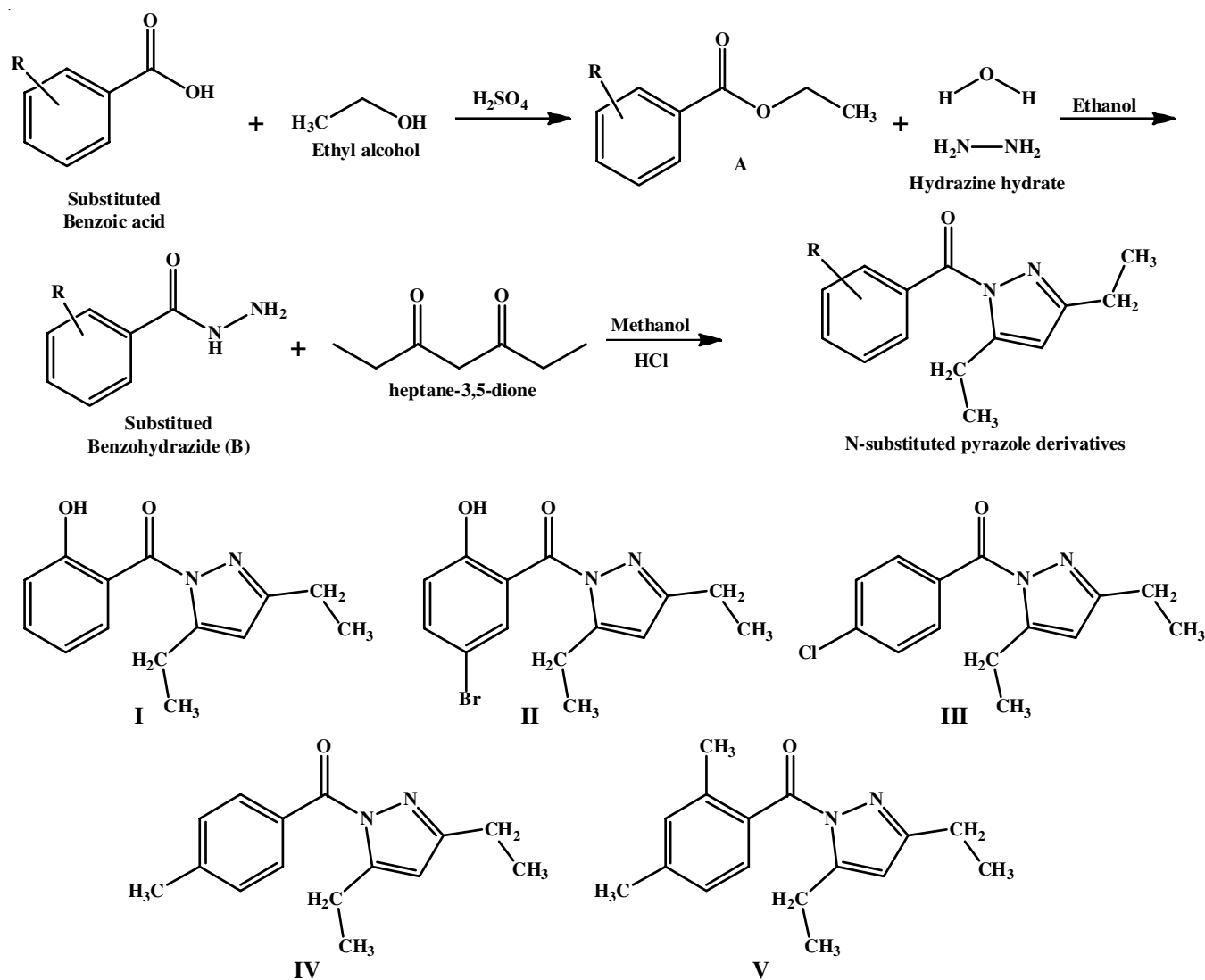
The synthesis of each compound was conducted according to the procedures outlined previously [13,14]. In this study, the solvents and reagents were of the highest grade and purchased from Merck, India. The reaction was tracked using thin-layer chromatography (TLC) on silica gel coated (Merck 60 F<sub>254</sub>) aluminum sheets with ethyl acetate:hexane (2:3) as mobile phase. The melting points were determined from electrothermal melting point instrument, the Stuart SMP10 (Barloworld Scientific Ltd., U.K.). The IR spectra were obtained in cm<sup>-1</sup> using a Shimadzu 8400S FTIR (Shimadzu Corporation, Japan). <sup>1</sup>H NMR (400.13 MHz) spectra acquired on a Bruker DRX-300 (300 MHz FT NMR) spectrophotometer with DMSO containing tetramethyl silane (TMS) as internal standard and <sup>13</sup>C NMR spectra were obtained at 126 MHz. The EI-MS data was

obtained using a Shimadzu high-resolution mass spectrometer. The analysis of carbon, hydrogen, oxygen and nitrogen was performed using a Perkin-Elmer 2400 Series-II CHN analyzer.

**Synthesis of substituted ethyl benzoate derivative (A):** Substituted benzoic acid (0.1 mmol) was mixed in absolute ethanol (60 mL) in the presence of 10 mL of H<sub>2</sub>SO<sub>4</sub>. The reaction mixture was refluxed under a water bath for 2 h. The TLC was employed to monitor the completion of the reaction, employing a mobile phase consisting of *n*-hexane and ethyl acetate.

**Synthesis of substituted benzohydrazide (B):** Absolute ethanol (50 mL) was refluxed with 0.01 mol of substituted benzoate and 0.02 mol of hydrazine hydrate for 18 h. The liquid was concentrated to half of its volume, cooled and then poured over crushed ice while being stirred for 3-4 h. After extracted from ethanol, the solid was filtered, dried and recrystallized.

**Synthesis of substituted (3,5-dimethyl-1H-pyrazol-1-yl)(phenyl)methanone derivatives:** A mixture of acid hydrazide, heptane-2,3-dione, 25 mL of methanol and 1 mL of conc. HCl was refluxed in a water bath for 10-12 h. The solution was then allowed to cool to room temperature and then recrystallized with absolute ethanol (**Scheme-I**).



**Scheme-I:** Schematic illustration synthetic pathway of N-substituted pyrazole derivatives

**((3,5-Diethyl-1H-pyrazol-1-yl)(2-hydroxyphenyl)-methanone) (compound I):** Yield: 84.5%; m.p.: 157-159 °C. Elemental anal. calcd. (found) %: C, 68.83 (68.84); H, 6.60 (6.65); N, 11.47 (11.50); O, 13.10 (13.1); IR (KBr,  $\nu_{\max}$ ,  $\text{cm}^{-1}$ ): 2850.07 (OH *str.*), 1631.84 (Ar-CH *bend.*), 1701.00 (C=O *str.*), 1543.91, 1190.7 (C=N *str.*);  $^1\text{H NMR}$  (500 MHz, DMSO)  $\delta$  ppm: 7.53 (s, 1H), 7.35 (s, 1H), 7.00 (s, 1H), 6.93 (s, 1H), 6.68 (s, 1H), 3.73 (s, 1H), 2.65-2.52 (m, 4H), 1.35-1.29 (m, 6H);  $^{13}\text{C NMR}$  (126 MHz, DMSO)  $\delta$  ppm: 170.31, 157.06, 155.82, 154.34, 134.70, 134.50, 129.99, 129.36, 129.30, 128.79, 128.02, 127.88, 127.26, 127.02, 126.63, 124.45, 123.71, 119.40, 119.01, 67.61, 64.87, 40.54, 20.89, 17.16; MS *m/z*: 244.12 ( $\text{M}^+$ ),  $\text{C}_{14}\text{H}_{16}\text{N}_2\text{O}_2$  (calcd.: 244.12);

**(5-Bromo-2-hydroxyphenyl)(3,5-diethyl-1H-pyrazol-1-yl)methanone (compound II):** Yield: 81.2%, m.p.: 151-153 °C. Elemental anal. calcd. (found) %: C, 52.03 (52.13); H, 4.68 (4.65); Br, 24.72 (24.75); N, 8.67 (8.65); O, 9.90 (9.89); IR (KBr,  $\nu_{\max}$ ,  $\text{cm}^{-1}$ ): 2849.21 (OH *str.*), 1628.13 (Ar-CH *bend.*), 1707.26 (C=O *str.*), 1564.34 (C=N *str.*), 1176.50 (C-N *str.*), 681.24 (C-Br *str.*).  $^1\text{H NMR}$  (500 MHz, DMSO)  $\delta$  ppm: 7.76 (d,  $J = 1.4$  Hz, 1H), 7.53 (dd,  $J = 7.5, 1.4$  Hz, 1H), 6.82 (d,  $J = 7.5$  Hz, 1H), 6.69 (s, 1H), 3.67 (s, 1H), 2.58 (q,  $J = 6.7$  Hz, 4H), 1.32 (dt,  $J = 11.8, 6.7$  Hz, 6H);  $^{13}\text{C NMR}$  (126 MHz, DMSO)  $\delta$  ppm: 170.31, 157.06, 155.82, 154.34, 134.70, 134.50, 129.99, 129.36, 129.30, 128.79, 128.02, 127.88, 127.26, 127.02, 126.63, 124.45, 123.71, 119.40, 119.01, 108.40, 107.37, 67.61, 64.87, 18.37, 17.16; MS *m/z*: 322.03 ( $\text{M}^+$ ),  $\text{C}_{14}\text{H}_{15}\text{BrN}_2\text{O}_2$  (calcd.: 322.19).

**(4-Chlorophenyl)(3,5-diethyl-1H-pyrazol-1-yl)methanone (compound III):** Yield: 84.5%, m.p.: 159-160 °C. Elemental anal. calcd. (found) %: C, 64.00 (64.10); H, 5.75 (5.70); Cl, 13.49 (13.50); N, 10.66 (10.68); O, 6.09 (6.10); IR (KBr,  $\nu_{\max}$ ,  $\text{cm}^{-1}$ ): 1567.22 (Ar-CH *bend.*), 1695.09 (C=O *str.*), 1510.81 (C=N *str.*), 1158.47 (C-N *str.*), 856.52 (C-Cl *str.*).  $^1\text{H NMR}$  (500 MHz, DMSO)  $\delta$  ppm: 7.64 (d,  $J = 7.5$  Hz, 2H), 7.46 (d,  $J = 7.5$  Hz, 2H), 6.69 (s, 1H), 2.58 (q,  $J = 6.7$  Hz, 4H), 1.32 (td,  $J = 6.7, 4.1$  Hz, 6H);  $^{13}\text{C NMR}$  (126 MHz, DMSO)  $\delta$  ppm: 168.50, 156.63, 148.92, 148.39, 125.64, 124.94, 123.24, 121.60, 109.19, 106.92, 106.34, 102.06, 20.90, 19.18, 17.77; MS *m/z*: 262.09 ( $\text{M}^+$ ),  $\text{C}_{14}\text{H}_{15}\text{ClN}_2\text{O}$  (calcd.: 262.09).

**(3,5-Diethyl-1H-pyrazol-1-yl)(*p*-tolyl)methanone (compound IV):** Yield: 76.85%; m.p.: 151-153 °C; Elemental anal. calcd. (found) %: C, 74.35 (74.40); H, 7.49 (7.50); N, 11.56 (11.60); O, 6.60 (6.66); IR (KBr,  $\nu_{\max}$ ,  $\text{cm}^{-1}$ ): 1597.62 (Ar-CH *bend.*), 1544.14 (C=O *str.*), 1487.15 (C=N *str.*), 1172.64 (C-N *str.*), 1295.38 ( $\text{C}_2\text{H}_5$  *str.*);  $^1\text{H NMR}$  (500 MHz, DMSO)  $\delta$  ppm: 7.65 (d,  $J = 7.5$  Hz, 2H), 7.31 (d,  $J = 7.5$  Hz, 2H), 6.69 (s, 1H), 2.58 (q,  $J = 6.7$  Hz, 4H), 2.35 (s, 3H), 1.32 (td,  $J = 6.7, 4.0$  Hz, 6H);  $^{13}\text{C NMR}$  (126 MHz, DMSO)  $\delta$  ppm: 168.50, 156.63, 137.77, 135.17, 128.98, 128.09, 126.06, 125.64, 124.94, 123.54, 123.24, 121.60, 65.51, 62.44, 19.18; MS *m/z*: 242.14 ( $\text{M}^+$ ),  $\text{C}_{15}\text{H}_{18}\text{N}_2\text{O}$  (calcd.: 242.14).

**(3,5-Diethyl-1H-pyrazol-1-yl)(2,4-dimethyl phenyl)methanone (compound V):** Yield: 83.45%; m.p.: 150-152 °C; Elemental anal. calcd. (found) %: C, 74.97 (74.98); H, 7.86 (7.90); N, 10.93 (10.95); O, 6.24 (6.25); IR (KBr,  $\nu_{\max}$ ,  $\text{cm}^{-1}$ ): 1632.81 (Ar-CH *bend.*), 1701.47 (C=O *str.*), 1539.87 (C=N *str.*), 1103.79

(C-N *str.*);  $^1\text{H NMR}$  (500 MHz, DMSO)  $\delta$  ppm: 7.60 (d,  $J = 7.5$  Hz, 1H), 7.26-7.16 (m, 2H), 6.69 (s, 1H), 2.58 (q,  $J = 6.7$  Hz, 4H), 2.35 (d,  $J = 11.7$  Hz, 6H), 1.32 (td,  $J = 6.7, 5.0$  Hz, 6H);  $^{13}\text{C NMR}$  (126 MHz, DMSO)  $\delta$  ppm: 170.30, 155.81, 154.37, 134.50, 130.00, 129.31, 128.03, 127.26, 127.03, 124.45, 119.01, 108.40, 64.86, 56.41, 18.07; MS *m/z*: 256.16 ( $\text{M}^+$ ),  $\text{C}_{16}\text{H}_{20}\text{N}_2\text{O}$  (calcd.: 256.16).

***In silico* Molecular docking studies:** Molecular docking studies were performed by using Autodock Vina software. Based on literature review, we selected HPV E6 [12] protein as a target for dock to the pyrazole derivatives. The HPV E6 was retrieved from the protein data bank (PDB ID:1DF5) and receptor was visualized by using Discovery Studio. The protein was dehydrated by removing the crystal water, then hydrogens were added, the protein was protonated and ionized. The energy was minimized using the Swiss-Protein Data Bank Viewer (SPDBV) force field. The activity of the protein was identified the amino acid in protein using Discovery Studio. The 3D optimization was performed on the molecule using Marvin Sketch after its creation and the .pdb file was saved. Once the data was obtained, the most favorable docking positions for each molecule were collected. The optimal position score values from the series were utilized to evaluate docking and interaction [15].

## Biological studies

***In vitro* cytotoxicity studies:** The sulforhodamine B (SRB) assay was used to determine the cytotoxicity of the synthesized compounds *in vitro* using the HeLa cell line. The HeLa cells were placed onto the 96-well flat-bottom plates at the appropriate cell count (3000 cells/180  $\mu\text{L}$ /well) and incubated overnight to facilitate adhesion. In quadruplicate, 20  $\mu\text{L}$  of pure chemicals were supplied with ultimate concentrations 10 times higher. Cells were then incubated for 72 h, first without any drugs and then with the treatments. Slight changes in the SRB assay as established by Skehan *et al.* [16,17] were applied to evaluate drug-induced cytotoxicity. After the medium was removed from the wells, the cells were fixed in 200  $\mu\text{L}$  of 10% cold TCA. After 30 min of incubation at 4 °C, the wells were cleaned five times with water. Each well contained 100  $\mu\text{L}$  of 0.4% SRB, which was left to stain the cells for 15 min. Plates were washed in 1% acetic acid to remove any unabsorbed colour and then dried overnight at room temperature. The air-dried plates were then shaken with 100  $\mu\text{L}$  of 10 mM tris base solution to solubilize the bound SRB. The  $\text{IC}_{50}$  value for each compound against each cell type was visually obtained by plotting the absorbance data. The half-life of cells treated with a drug was determined compared to those that were untreated.

***In vivo* studies:** The effectiveness of the synthesized compounds against a Dalton's Lymphoma mice ascites tumor model was also evaluated.

**Animals:** The animal house at Saveetha College of Pharmacy provided a healthy population of Swiss Albino mice weighing  $2 \pm 2.0$  g. Prior to any experiments, each animal's body mass was recorded. The animals were kept under conventional conditions including a 12 h dark/12 h light cycle and a temperature of 2 °C. Nutritionally complete pellets were used to nourish the mice.

**Model of Dalton's lymphoma with ascites tumour:** An ascites tumour model in mice was used to assess the efficacy of the synthesized compounds. Swiss albino mice developed Dalton's lymphoma ascites cells after receiving an intraperitoneal injection of  $1 \times 10^5$  cells/mL. On day 11 after tumour transplantation, while the tumour was in its log phase, the fluid was aseptically drained from the intraperitoneal cavity, removing the cells from the tumour. Three times, centrifugation at 300-400 rpm was used to wash the ascitic fluid with phosphate buffer saline (PBS) and then all supernatant was discarded. Normal saline was used to dilute the cells. A hemocytometer was used to count tumor cells by excluding the trypan blue dye. A  $1 \times 10^5$  cells were obtained in 0.1 mL of PBS after diluting the cell suspension. Treatment was started 24 h after injecting tumor cells into the peritoneal cavities of the animals. The cytotoxic effectiveness of test sample was compared to that of 5-fluorouracil (20 mg/kg) and DAL controls after 14 days of once-daily treatment.

Five mice each were randomly assigned to one of four experimental groups.

**Group-1:** The control group consists of the DAL-bearing mice.

**Group 2:** Mice with DAL were given the normal intraperitoneal treatment of fluorouracil at a dose of 20 mg/kg.

**Group 3:** Mice with DAL that were given 50 mg/kg of compound C.I. intraperitoneally.

**Group 4:** Compound C.II was administered intraperitoneally to mice carrying DAL at a dose of 50 mg/kg.

10 days of intraperitoneal administration of both the control and experimental drugs was conducted. In the group given a placebo, the concentration of CMC was 0.25%.

**Body weight analysis:** All the mice were weighed daily, after tumor inoculation. The average gain in body weight was determined and recorded and the % increase in body weight was calculated as follows [18]:

$$\text{Increase in body weight} = \frac{A - B}{A} \times 100$$

where A = gain in body weight of control group; B = gain in body weight of treated group.

**Determination of mean survival time (MST):** From the day of tumor injection, the entire amount of days an animal lived was recorded. The mean survival time (MST) was established through observation of the lifespan of mice with tumors [19]. The average number of years people in each treatment group lived was also determined.

$$\text{MST} = \frac{\sum \text{Survival time (days) of each mice in a group}}{\text{Total number of mice}}$$

**Determination of percentage increase in life span (% ILS):** The formula computed the percentage increase in longevity based on the mean survival rate.

$$\text{ILS (\%)} = \frac{\text{MST of treated group} - \text{MST of control group}}{\text{MST of treated group}} \times 100$$

**Histopathological analysis:** The animals were euthanized by surgically dislocating their cervical vertebrae. After removing the liver from the slaughtered animals, it was preserved by

being fixed in 10% phosphate-buffered formalin, dried in alcohol and finally embedded in paraffin. The histopathological evaluations involved cutting paraffin blocks into sections of a specific thickness and stained them with hematoxylin and eosin. The tissue segments were examined using a light microscope.

**Estimation of haematological parameters:** In order to study the hematological changes associated with drugs administered different blood parameters like RBC count, WBC count and total leukocyte count and hemoglobin level were estimated for control groups and plant-extracted treated groups. On day 21 of trial, blood was taken from the retro-orbital plexus. Average and standard values were used to make comparisons [20].

**Preparation of blood serum:** Diethyl ether was administered to induce anesthesia in the animals following a 21-day period of treatment-induced starvation. Using a capillary tube, blood was drawn from the eye (retro-orbital haemorrhage) all the way to the maximum level. After that, the animals were killed by dislocating their cervical spines and the fluid from inside their brains was measured. A blood sample was taken in order to calculate the percentage of red blood cells, white blood cells and haemoglobin.

**Viable and non-viable cell count:** Diethyl ether was administered to induce anesthesia in the animals following 21 days of treatment. In the intraperitoneal cavity, we retrieved approximately 0.2 mL of cell suspension using a syringe. We then combined this with 0.1 mL of 0.4% trypan blue, 0.1 mL of normal saline or 0.1 mL of PBS and allowed to stand ideal for at least 5 min. A single drop of the solution was then transferred to a Neubauer chamber and covered with a glass slide. Cell viability was determined by viewing the compartment under a microscope. The live cells stand out as white on the blue backdrop, whereas the dead cells were shaded in a dark blue [21]. A formula was used to obtain the total number of cells.

$$\text{Cell count} = \text{No. of cells} \times \text{Dilution factor} \times \text{Volume factor}$$

**Statistical analysis:** One-way ANOVA was used for the statistical testing. The data was summarized as a mean standard error of the mean. A significance level of  $p < 0.05$  was used to identify differences.

## RESULTS AND DISCUSSION

**Scheme-I** depicts the synthesis of a novel series of N-substituted pyrazole derivatives, which were characterized through TLC, IR,  $^1\text{H}$  NMR,  $^{13}\text{C}$  NMR and mass spectrometry. The existence of a hydroxyl (OH) group in compounds **I** and **II** was established by an IR absorption peak at  $2850\text{ cm}^{-1}$  and the presence of a ketonic group (C=O) in the pyrazole scaffold was confirmed by an IR absorption peak at  $1701\text{ cm}^{-1}$ . The (C-H) group in the aromatic ring was appeared around  $1628\text{--}1597\text{ cm}^{-1}$  in the spectra of compounds **I-V**. The C=N stretching, which is characteristic of the pyrazole skeleton, was detected in the  $1590\text{--}1400\text{ cm}^{-1}$  region of the spectrum. The presence of a C-Br group is confirmed by the  $680\text{--}610\text{ cm}^{-1}$  region of compound **II**. In compound **III**, the peak at  $856\text{--}830\text{ cm}^{-1}$  is attributed to a C-Cl group. The molecular ion peaks ( $M^+$ ) were analyzed in the mass spectra of the substances and

found to be constant. The optimal aromatic proton concentration ranges from  $\delta$  6.93 to 6.68 ppm. The appearance of singlet protons in  $^1\text{H}$  NMR spectra within the range of 3.46 to 4.5 ppm is due to the existence of the  $-\text{NH}-$  group. An aromatic methyl group suggested by a singlet proton at 2.52-2.65 ppm for each proton in its  $^1\text{H}$  NMR spectra, definitively establishes the presence of pyrazole molecules.

**Molecular docking studies:** Molecular docking models of synthesized pyrazole derivatives revealed significant interactions, providing direction for the selection of synthesized derivatives for enhanced anticancer efficacy. Docking the constructed structures into the HPV E6 active site allowed to ascertain if the synthesized compounds displayed the same interactions as recognized HPV E6 inhibitors. Hydrogen bond interaction between the NH of pyrazole ring and the OH group was observed during docking of compound **I**. Hydrophobic interaction between  $\text{CH}-\text{CH}_3$  and the benzene ring is seen in GLN A:22, VAL A:25, TRP A:26, HIS A:19 and LEU A:23. And LYS A:29 wrapped the benzene ring entirely. Compound **II** (ILE A:55, ILE A:14 and TRY A:51) exhibited a benzene-pyrazole hydrophobic interaction. Amino acids VAL A:25, GLN A:18, THR A:52, ILE A:48 and GLU A:47 is surrounded by these others. In addition to being flanked by GLNA:18, THRA:52 and GLU A:47, compound **III** also had three hydrophobic bond interactions (benzene ring ILE A:14 and a:55, pyrazole ring ILE A:48, LEU A:21 and TRY A:51). Interactions between the benzene and pyrazole rings were observed in

compound **IV** at TYR A:51, ILE A:48, LEU A:21 and VAL A:25). The amino acids ILE A:55, THRA:52, GLNA:18, GLN A:22 and GLU A:47 form the outermost portion. Three hydrophobic bond interactions were observed in compound **V** (benzene ring ILE A:55 and A:14, pyrazole ring ILE A:48 and TRY A:51). There were also GLNA:18, THRA:52 and GLU A:47 in the vicinity of the compound. The results obtained in anti-angiogenesis, *in vitro* and *in vivo* cancer activity suggest that the introduction of  $-\text{OH}$  in the benzene ring of compounds **I** and **II** contributed to additional hydrogen bond interactions with the active site amino acids of HPV E6, which may have contributed to the better activity of these compounds as compared to other compounds **III**, **IV** and **V**. Table-1 shows the docking energy values of HPV E6's interaction with the amino acids in its active site. Fig. 1 shows 2D depictions of compounds **I-V**.

**In vitro anticancer activity (SRB assay):** Half-maximal inhibitory concentration ( $\text{IC}_{50}$ ) values for the three most cytotoxic compounds **I**, **II** and **III** were determined to be 29.74, 28.17 and 21.78  $\mu\text{g}/\text{mL}$ , respectively (Table-2). Compounds **IV** and **V** have low to moderate activity (67.05 and 56.66  $\mu\text{g}/\text{mL}$ , respectively). More activity is shown when the hydroxyl group ( $\text{OH}$  group) is substituted for the *ortho*-position, whereas Cl and Br are substituted for the *para*-position. An improvement in activity is consistent with an raise in hydrophobicity at the substituted ring while a reduction in activity is consistent with an increase in hydrophilicity.

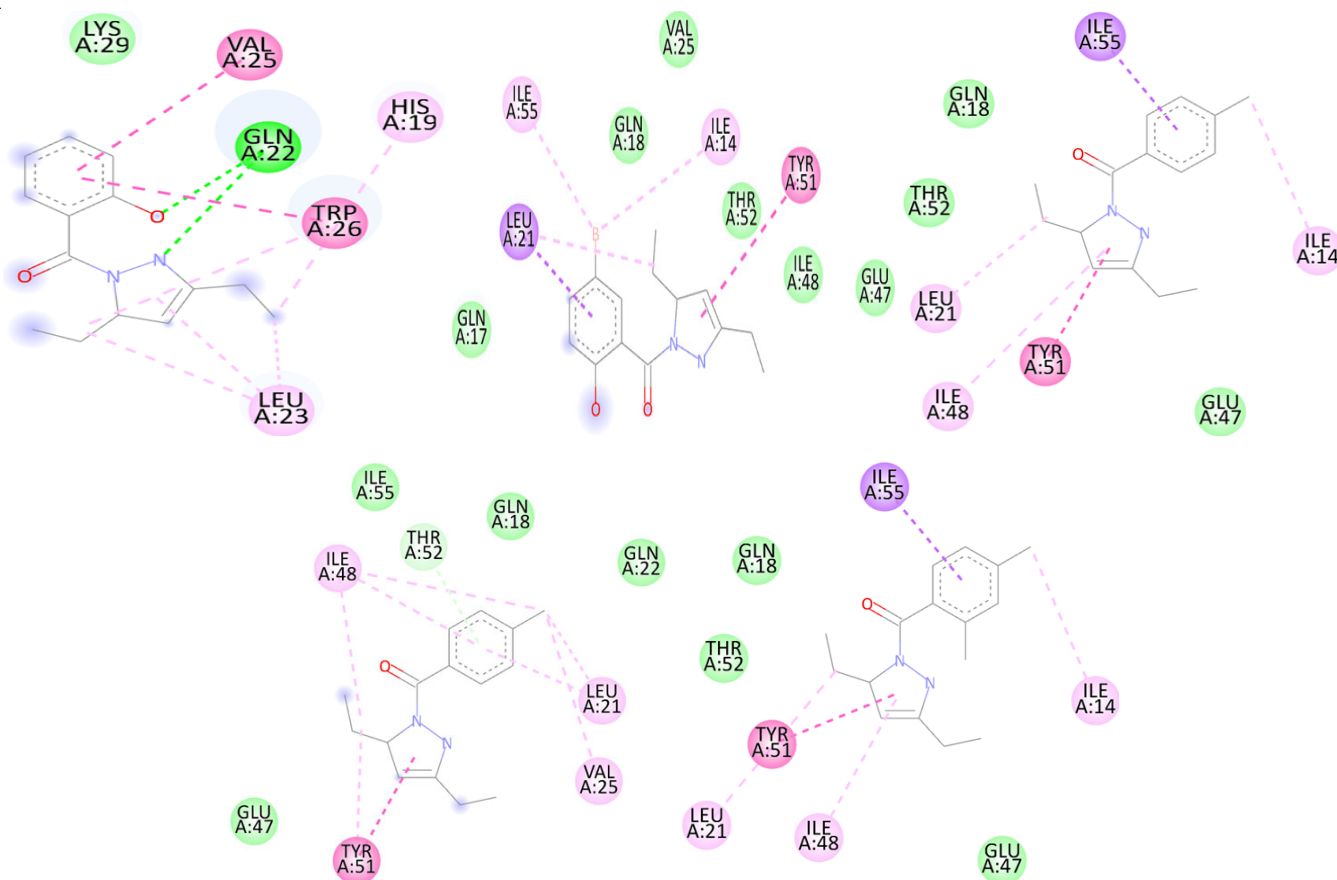


Fig. 1. Two-dimensional interaction of compounds **I-V** bound to HPV E6 active site (PDB ID: 1DF5)

TABLE-1  
DOCKING ENERGIES OF NOVEL N-SUBSTITUTED PYRAZOLE  
DERIVATIVES WITH ACTIVE SITE AMINO ACIDS OF HPV E6 RECEPTOR

| Compounds  | Binding energy (Kcal/mol) | Active site amino acids   |
|------------|---------------------------|---|
| <b>I</b>   | -5.6                      | GLN A:22, VAL A:25, TRP A:26, HIS A:19, LEU A:23, LYS A:29  |
| <b>II</b>  | -5.5                      | ILE A:55, ILE A:14 and TRY A:51, VAL A:25, GLN A:18, THR A:52, ILE A:48, GLU A:47, GLNA:18, THRA:52, GLU A:47 |
| <b>III</b> | -5.8                      | ILE A:14,55, ILE A:48, LEU A:21, TRY A:51, GLN A:18, THR A:52, GLU A:47.                                      |
| <b>IV</b>  | -5.1                      | TYR A:51, ILE A:48, LEU A:21, VAL A:25. ILE A:55, THR A:52, GLN A:18, GLN A:22, GLU A:47                      |
| <b>V</b>   | -5.0                      | ILE A:55, A:14, ILE A:48, TRY A:51, GLNA:18, THRA:52, GLU A:47  |

TABLE-2  
IC<sub>50</sub> VALUES OF SYNTHESIZED  
COMPOUNDS I-V IN SRB ASSAY

| Compd.    | Tested conc. (µg/mL) | OD at 540 nm (mean OD) | Viability (%) | IC <sub>50</sub> |
|-----------|----------------------|------------------------|---------------|------------------|
| <b>C1</b> | 100                  | 0.151                  | 25.91         | 29.74            |
|           | 80                   | 0.183                  | 31.39         |                  |
|           | 40                   | 0.265                  | 45.46         |                  |
|           | 20                   | 0.297                  | 50.96         |                  |
|           | 10                   | 0.350                  | 60.04         |                  |
|           | Control              | 0.580                  |               |                  |
| <b>C2</b> | 100                  | 0.518                  | 89.41         | 28.17            |
|           | 80                   | 0.673                  | 83.97         |                  |
|           | 40                   | 0.799                  | 62.75         |                  |
|           | 20                   | 0.890                  | 46.56         |                  |
|           | 10                   | 0.920                  | 41.38         |                  |
|           | Control              | 0.580                  |               |                  |
| <b>C3</b> | 100                  | 0.415                  | 71.55         | 21.78            |
|           | 80                   | 0.655                  | 84.07         |                  |
|           | 40                   | 0.712                  | 77.25         |                  |
|           | 20                   | 0.845                  | 54.32         |                  |
|           | 10                   | 0.912                  | 42.76         |                  |
|           | Control              | 0.580                  |               |                  |
| <b>C4</b> | 100                  | 0.420                  | 72.41         | 67.05            |
|           | 80                   | 0.567                  | 97.75         |                  |
|           | 40                   | 0.764                  | 68.28         |                  |
|           | 20                   | 0.821                  | 61.24         |                  |
|           | 10                   | 0.912                  | 42.76         |                  |
|           | Control              | 0.580                  |               |                  |
| <b>C5</b> | 100                  | 0.315                  | 54.31         | 56.66            |
|           | 80                   | 0.490                  | 84.48         |                  |
|           | 40                   | 0.730                  | 74.14         |                  |
|           | 20                   | 0.859                  | 67.18         |                  |
|           | 10                   | 0.925                  | 40.52         |                  |
|           | Control              | 0.580                  |               |                  |

***In vivo* anticancer activity:** Table-3 presents data of body weight gain, average surviving time and percentage increase in lifespan as measures of the anticancer efficacy in mice with DAL tumours. Table-4 shows the results of a screening using

measures of hematological parameters, including viable and non-viable cell count. The *in vivo* screening parameters revealed that all drugs had a substantial impact compared to the control. Compounds **I**, **II** and **III**, however, distinguished out from the others due to their exceptional antitumor potential. Most chemotherapy drugs have not significantly expanded life duration and they have also caused additional adverse effects, making increasing longevity a crucial component in cancer therapy. Therefore, the synthesized compounds were superior to the control in terms of longevity. Mice who had DAL injected into them gained weight significantly between days 0 and 11 and again on day 12 ( $5.02 \pm 0.815$ ). When compared to the control group, the average drugs resulted in  $3.35 \pm 0.0552$ . A dosage of 50 mg/kg of compound **III** significantly decreased body weight as indicated in Table-3.

**Hematological parameters and viable and non-viable cells:** The newly synthesized compounds were compared to the control in every hematological parameter study. In pyrazole-treated rats, red blood cell (RBC) levels increased dramatically but abnormally compared to controls. Although all three compounds increase the RBC count as not effective as standard. Pyrazole derivatives treated groups had significantly reduced numbers of white blood cells (WBCs). Mice given newly synthesized compounds did not show an increase in hemoglobin levels.

The mice were euthanized after 21 days of treatment. The cells from the intraperitoneal cavities were collected from both the experimental and control groups. The cells were then treated with trypan blue solution and diluted with normal saline for NMT 1 min. The solution was then observed under a microscope by loading on a Neubauer chamber. Both the number of live and dead cells were counted. In Fig. 2, the living cells are shown as white on a blue background, whereas dead cells are displayed in a darker shade of blue.

In the groups that were given the drugs, the number of live cells fell. In comparison to the control, the proportion of dead

TABLE-3  
BODY WEIGHT GAIN, MEAN SURVIVAL TIME AND EFFECT OF SYNTHETIC PYRAZOLE COMPOUNDS ON DAL-BEARING MICE

| Compounds           | Dose (mg/kg) | Increase in body weight (%) | Increase in lifespan (%) | MST (days)      |
|---------------------|--------------|-----------------------------|--------------------------|-----------------|
| Control             | 30           | –                           | –                        | 21.20 ± 0.30    |
| Std. (fluorouracil) | 20           | 3.35 ± 0.0552               | 80.33                    | 38.23 ± 0.56*** |
| Compound <b>I</b>   | 50           | 5.02 ± 0.0815**             | 44.62                    | 34.66 ± 1.9**   |
| Compound <b>II</b>  | 50           | 4.36 ± 0.0593**             | 44.95                    | 30.53 ± 1.8**   |
| Compound <b>III</b> | 50           | 3.89 ± 0.0778*              | 57.54                    | 33.54 ± 0.52**  |

Data expressed as mean ± SEM of five animals; Statistical analysis was performed by student 'T' test \*\*\* $p < 0.01$ , \*\* $p < 0.05$ .

TABLE-4  
BLOOD TEST RESULTS, CELL VIABILITY AND THE IMMUNE SYSTEM OF  
MICE GIVEN DAL AS A TREATMENT FOR PYRAZOLE DERIVATIVES

| Treatment    | RBC (million/ $\mu\text{M}^3$ ) | Total WBC ( $1 \times 10^3 \mu\text{M}^3$ ) | Hb (g/dl)              | Viable cell count     | Non-viable cell count |
|--------------|---------------------------------|---|------------------------|-----------------------|-----------------------|
| Control      | $4.33 \pm 0.15^*$               | $14.33 \pm 0.13^{**}$                       | $8.33 \pm 0.66^*$      | $9.77 \pm 0.17$       | $0.84 \pm 0.10$       |
| Standard     | $10.12 \pm 0.77^{***}$          | $11.37 \pm 0.81^*$                          | $12.16 \pm 0.49^*$     | $2.28 \pm 0.07^{***}$ | $5.75 \pm 0.07^{***}$ |
| Compound I   | $8.32 \pm 0.15^{**}$            | $11.16 \pm 0.13^*$                          | $10.21 \pm 0.23^{***}$ | $4.583 \pm 0.21^{**}$ | $4.783 \pm 0.19^{**}$ |
| Compound II  | $7.04 \pm 0.17^*$               | $12.31 \pm 0.37^*$                          | $9.53 \pm 0.29$        | $3.254 \pm 0.12^{**}$ | $3.873 \pm 0.12^{**}$ |
| Compound III | $8.04 \pm 0.17^*$               | $11.12 \pm 0.37^*$                          | $10.13 \pm 0.29$       | $4.500 \pm 0.22^{**}$ | $4.600 \pm 0.25^{**}$ |

On day 21 of the trial, values are shown as the mean  $\pm$  SEM (n = 6), with  $***p < 0.001$  and  $**p < 0.01$ , respectively, based on a comparison between the treated group and the DAL control group.

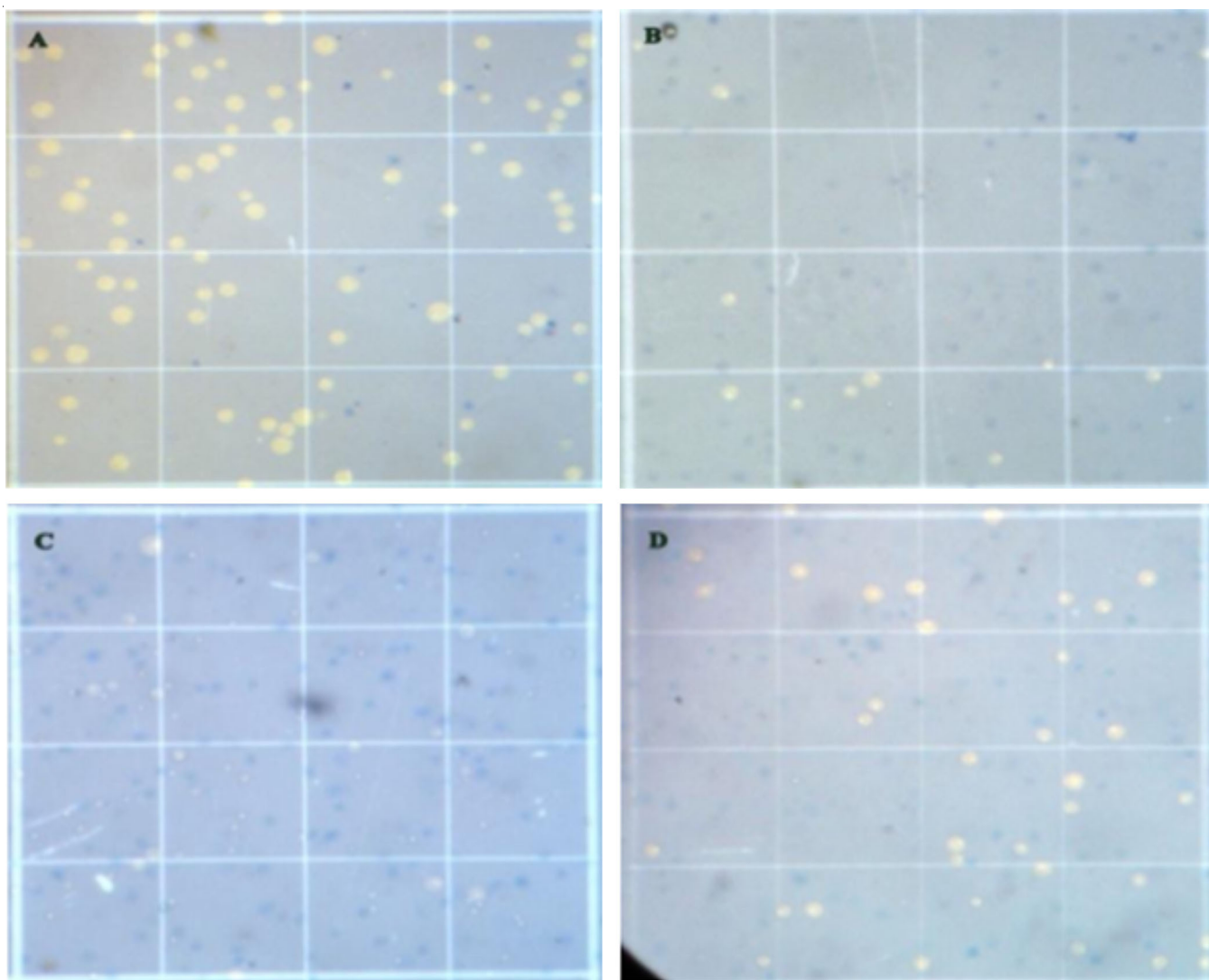


Fig. 2. Effect of pyrazole derivative on viable and non-viable cells

cells is higher in the pyrazole-treated groups, which demonstrates that pyrazole derivative treatment inhibits the metastasis of DAL tumour cells in animal models.

**Histopathological studies:** On 21<sup>st</sup> day, the animals were sacrificed. Liver and kidney were isolated and after suitable preparation, the histology of the tissues of control and treated groups were analyzed under a 40x of light microscope. Cellular infiltration and modest central venous dilatation were seen on histological examinations of liver tissue from the control group

of mice. Central vein dilatation in the hepatocyte tissue of the groups receiving treatment was minimal, indicating less hepatotoxicity than in the control group (Fig. 3).

The presence of -OH and -Cl groups at benzene ring may be responsible for the high *in vivo* anticancer activity of compounds I and III. The inclusion of an electron-withdrawing group, such as 2-OH or 4-chloro group, improves the performance of compounds I and III significantly relative to the control, but their activity is lower than that of standard. When

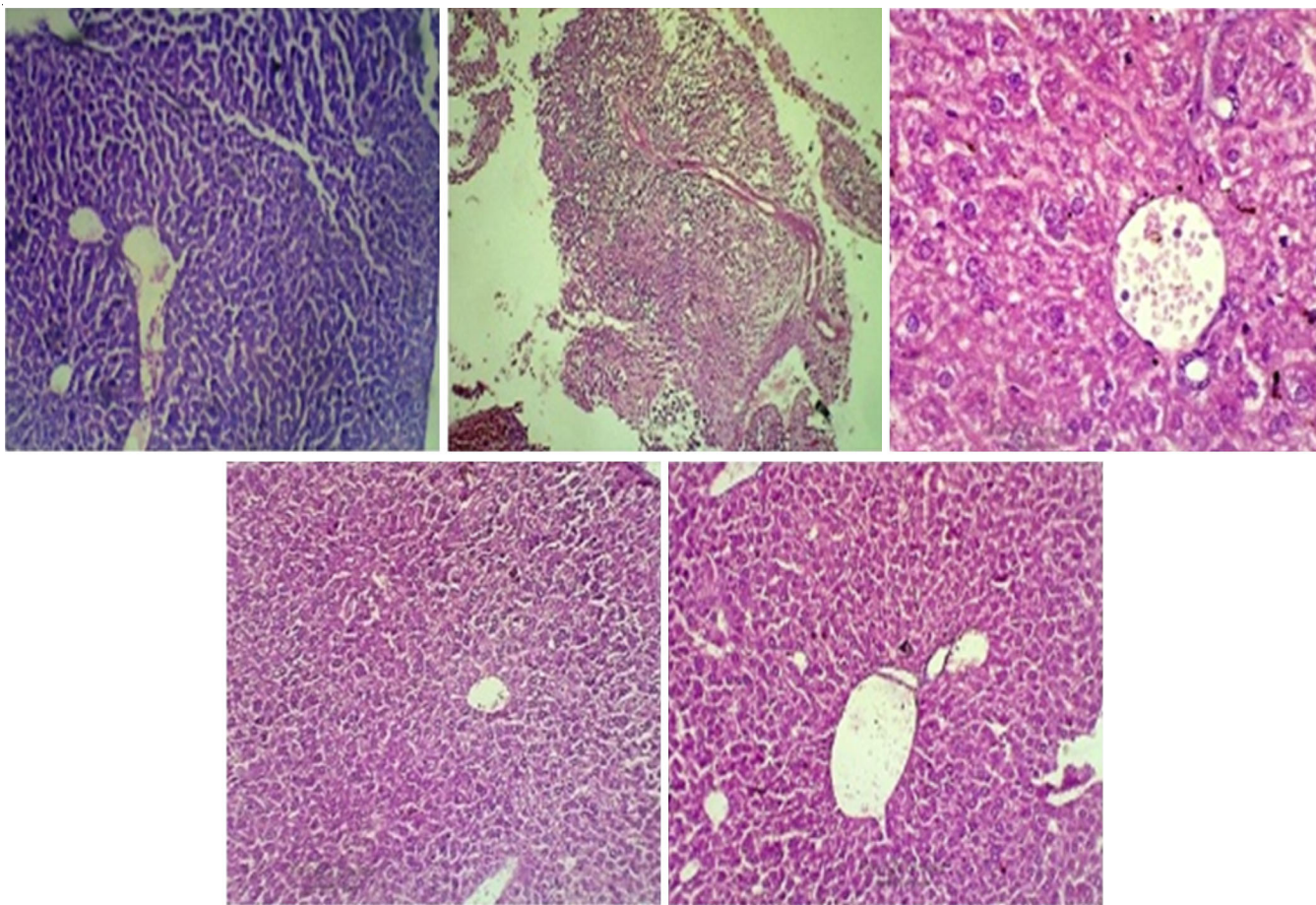


Fig. 3. Histopathology images of liver and kidney after treatment with synthetic pyrazole derivatives

these groups are added to the pyrazole skeleton, the anticancer activity is lowered to a moderate level. Treatment with many synthetic pyrazole derivatives reversed the abnormal haematological parameters in this study. Pyrazole scaffold thus proved to have a protective role in hemopoiesis. The compounds induced a decrease in both the population of living cells and the population of dead cells. These results demonstrated the connection between tumor cells and pyrazole derivatives, a group of chemotherapeutic drugs, which annihilate cancer cells through a direct cytotoxic mechanism.

### Conclusion

Few novel N-substituted pyrazole derivatives (**I-V**) were synthesized and characterized. The anticancer activity of the pyrazole derivatives highlighted the importance of the OH and Cl group in the benzene at the N-substituted pyrazole scaffold. Compounds **I** and **III** are shown to have effective therapeutic efficacy, suggesting that they might serve as a foundation for the development of less toxic anticancer compounds based on the same pyrazole scaffold.

### CONFLICT OF INTEREST

The authors declare that there is no conflict of interests regarding the publication of this article.

### REFERENCES

- U.T. Sankpal, H. Pius, M. Khan, M.I. Shukoor, P. Maliakal, C.M. Lee, M. Abdelrahim, S.F. Connelly and R. Basha, *Tumour Biol.*, **33**, 1265 (2012); <https://doi.org/10.1007/s13277-012-0413-4>
- S. Adel, E. Azab, A. Mohamed, A. Omar, A.M. Alaa, I. Naglaa et al., *Eur. J. Med. Chem.*, **45**, 9 (2010).
- Y. Gao, K.J. Shen, L. Milane, J. Hornicek, M. Amiji and Z. Duan, *Curr. Med. Chem.*, **22**, 1335 (2015); <https://doi.org/10.2174/0929867322666150209151851>
- T. Brzozowski, *Curr. Med. Chem.*, **19**, 2 (2012); <https://doi.org/10.2174/092986712803414024>
- S.T. Al-Rashood, I.A. Aboldahab, M.N. Nagi, L.A. Abouzeid, A.A.M. Abdel-Aziz, S.G. Abdel-hamide, K.M. Youssef, A.M. Al-Obaid and H.I. El-Subbagh, *Bioorg. Med. Chem.*, **14**, 24 (2006); <https://doi.org/10.1016/j.bmc.2006.08.030>
- F. Sams-Dodd, *Drug Discov. Today*, **18**, 211 (2013); <https://doi.org/10.1016/j.drudis.2012.10.010>
- X. Sun, S. Vilar and N.P. Tatonetti, *Sci. Transl. Med.*, **5**, 205 (2013); <https://doi.org/10.1126/scitranslmed.3006667>
- P.N. Dube, S.S. Bule, S.N. Mokale, M.R. Kumbhare, P.R. Dighe and Y.V. Ushir, *Chem. Biol. Drug Des.*, **84**, 409 (2014); <https://doi.org/10.1111/cbdd.12324>
- B. Maggio, D. Raffa, M.V. Raimondi, F. Plescia, M.L. Trincavelli, C. Martini, F. Meneghetti, L. Basile, S. Guccione and G. Daidone, *Eur. J. Med. Chem.*, **54**, 709 (2012); <https://doi.org/10.1016/j.ejmech.2012.06.028>
- A. Ahmad, H. Varshney, A. Rauf, F.M. Husain and I. Ahmad, *J. King Saud Univ. Sci.*, **26**, 290 (2014); <https://doi.org/10.1016/j.jksus.2013.09.003>



11. N. Das, A. Verma, P.K. Shrivastava and S.K. Shrivastava, *Indian J. Chem.*, **47B**, 1555 (2008).
12. E.K. Yim and J.S. Park, *Cancer Res. Treat.*, **37**, 319 (2005); <https://doi.org/10.4143/crt.2005.37.6.319>
13. P.N. Dube, S.S. Bule, Y.V. Ushir, M.R. Kumbhare and P.R. Dighe, *Med. Chem. Res.*, **24**, 1070 (2015); <https://doi.org/10.1007/s00044-014-1201-z>
14. N.V. Patel and D.J. Sen, *Am. J. Adv. Drug Deliv.*, **1**, 2 (2013).
15. A. Garofalo, L. Goossens, P. Six, A. Lemoine, S. Ravez, A. Farce and P. Depreux, *Bioorg. Med. Chem. Lett.*, **21**, 2106 (2011); <https://doi.org/10.1016/j.bmcl.2011.01.137>
16. P. Skehan, R. Storeng, D. Scudiero, A. Monks, J. McMahon, D. Vistica, J.T. Warren, H. Bokesch, S. Kenney and M.R. Boyd, *J. Natl. Cancer Inst.*, **82**, 1107 (1990); <https://doi.org/10.1093/jnci/82.13.1107>
17. A. Monks, D. Scudiero, P. Skehan, R. Shoemaker, K. Paull, D. Vistica, C. Hose, J. Langley, P. Cronise, A. Vaigro-Wolff, M. Gray-Goodrich, H. Campbell, J. Mayo and M. Boyd, *J. Natl. Cancer Inst.*, **83**, 757 (1991); <https://doi.org/10.1093/jnci/83.11.757>
18. A.E. Eckhardt, B.N. Malone and I.J. Goldstein, *Cancer Res.*, **42**, 2977 (1982).
19. M.P. Sathisha, V.K. Revankar and K.S.R. Pai, *Met. Based Drugs*, **2008**, 362105 (2008); <https://doi.org/10.1155/2008/362105>
20. A. Mukherjee, S. Dutta and U. Sanyal, *J. Exp. Clin. Cancer Res.*, **26**, 489 (2007).
21. S. Kameshwaran, V. Suresh, G. Arunachalam, S.K. Kanthlal, M. Mohanraj, *Int. Res. J. Pharm.*, **3**, 246 (2012).